NANO LETTERS

2004
Vol. 4, No. 3
483−486

Nanowire and Mesh Conformations of Diblock Copolymer Blends at the Air/Water Interface

Young-Soo Seo,*,† K. S. Kim,† Arielle Galambos,‡ R. G. H. Lammertink,§ G. J. Vancso,§ J. Sokolov,† and M. Rafailovich†

Material Science & Engineering, SUNY at Stony Brook, Stony Brook, New York 11779, Wellesley College, Wellesley, Massachusetts 02481, and University of Twente, Faculty of Chemical Technology, 7500 AE Enschede, The Netherlands

Received October 21, 2003; Revised Manuscript Received December 12, 2003

ABSTRACT

We investigated the structures formed when blends of poly(styrene-*b*-ferrocenyl silane) (PS-*b*-FS) and poly(styrene-*b*-2-vinyl pyridine) (PS-*b*-P_2VP) were spread at the air/water interface. The results demonstrated that new structures were formed which were distinct from those formed when either of the copolymers was spread alone. Furthermore, in contrast to the pure copolymer films, the morphologies could also be controlled with surface pressure and applied external electric fields. This greatly increases the range of nanostructured patterns that could be produced by this technique in the fabrication of polymeric templates for lithography.

Recently, self-assembly of inorganic or organic materials has attracted much attention in developing various nanosized structures. These structures can be used as masks on various substrates enabling inexpensive lithographic techniques for the development of nanoscale devices. Diblock copolymers are currently favored for applications using self-assembly because the morphology of the structures produced can be controlled by varying the molecular weight and relative length of each block and the orientation can be controlled by application of electric fields.[1] The creation of self-assembled structures for the melt can prove challenging since it requires high temperatures (well above glass transition temperature, T_g) and long annealing times in very good vacuum. In addition, the structures obtained are dependent on the polymer−substrate interactions which can be difficult to control.

The air/water interface offers an easier medium for achieving diblock copolymer self-assembly because it is well characterized and can be done at ambient temperatures. On the other hand, much less is known regarding the structures that are formed. Several authors[2−4] have shown that diblock copolymers form surface micelles where the hydrophilic block forms a brush anchored at the surface by the hydrophobic core. They also demonstrated that a phase diagram, analogous to the one in the melt, can also be created where different morphologies are generated by varying the ratio of the two blocks. Lennox et al.[5] demonstrated that the dimensions of these structures can be further adjusted by the addition of homopolymers.

In the melt it is well known that morphology can be controlled through blending of polymers. Here we discuss the structures formed when two block copolymers are blended and then spread together at the air/water interface. We discuss systematically the structures formed as a function of the ratio between the blocks and show how one can create a dense network of nanoscale wires which can be further condensed into a mesh through the in-situ application of low external electric fields (<100 V/cm) after spreading.

The system we chose to study is symmetric monodisperse diblock copolymer of poly(styrene-*b*-ferrocenylsilane) (PS-*b*-FS, $N_{PS}/N_{FS} = 54/52$), where the poly(ferrocenyl silanes) consist of alternating ferrocene and silane units in the main chain.[6−7] This block is a member of the organometallic class of polymers that has attracted considerable attention recently because of their unique electrical, magnetic, and optical characteristics.[8] Because both PS and FS blocks are hydrophobic, the copolymer cannot be spread at the air/water interface. We therefore blended it with poly(styrene-*b*-2-vinyl pyridine) (PS-*b*-P_2VP, $N_{PS}/N_{P2VP} = 1k/1k$) where we postulated that the pyridine unit would spread at the air/water interface while the PS blocks would mix and bind the two copolymers.

The films were produced by dissolving in chloroform different fractions of the two copolymers for obtaining a total

* Corresponding author. Present address: NCNR, NIST. Email: ysseo@nist.gov.
† SUNY at Stony Brook.
‡ Wellesley College.
§ University of Twente.

10.1021/nl034917i CCC: $27.50
Published on Web 12/24/2003

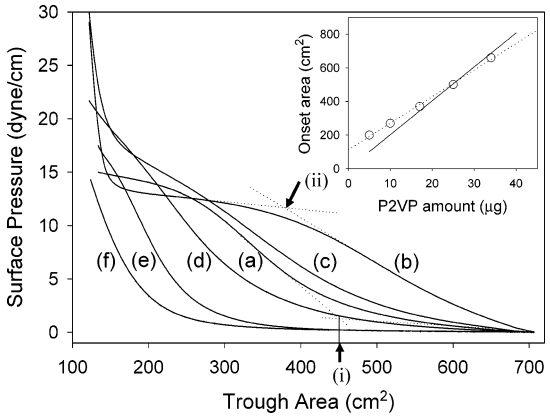

Figure 1. Π−A diagrams of PS-*b*-PF and PS-*b*-P_2VP block copolymers blends (SF/SP) as a function of blend composition at the air/water interface. (SF/SP) = (a) 0:1; (b) 1:2; (c) 1:1; (d) 2:1; (e) 4:1; (f) 5:1. Onset area (i) and onset point of plateau (ii) are indicated by arrows. The onset area for (a) should be doubled in order to compare quantitatively with the blends onset area because spreading solution volumes for (a) are 50 μL and the others are 100 μL in the same solution concentration of 1 mg/mL. (Inset) Open circles indicate the onset area for each blend with dotted guide line. Total cross-sectional area of VP monomer calculated (see text) is in solid line.

polymer concentration of 1 mg/mL. The solution was spread on a KSV Langmuir trough with a maximum area of 704 cm^2 at 20 °C, using distilled and deionized water (Millipore) as the subphase. The film was allowed to spread for approximately 10−15 min before pressure−area (Π−A) isotherms were recorded or LB films were lifted at barrier and dipper speed of 2 mm/min, respectively.

The Π−A isotherms on the water surface of the PS-*b*-FS and PS-*b*-P_2VP blend (SF/SP) monolayers are plotted in Figure 1 for different SF/SP ratios. The isotherm labeled (a), where the maximum onset area indicated by arrow (i) is obtained (see figure caption), corresponds to a pure PS-*b*-P_2VP copolymer solution where the hydrophobic PS phase is aggregated while hydrophilic P_2VP phase wets the water surface and is responsible for the increase in the surface pressure. The isotherm has two characteristic features, an onset area and a distinct plateau region. At the other extreme, no isotherm could be obtained for the pure PS-*b*-FS copolymers since both blocks are hydrophobic when spread at the air/water interface, no increase in surface pressure could be obtained with decreasing surface area.

In the figure we also plot the isotherms for the copolymer blends where the PS-*b*-P_2VP fraction is decreased from 100% to 17%. From the figure we can see that the onset point of the plateau indicated by arrow (ii) decreases with increasing PS-*b*-FS fraction and disappears for fractions smaller than 33%, indicating that the films are becoming softer or more compressible.

From the figure we can see that the onset area for the pure PS solution is ∼450 cm^2 when 50 μL of a 1 mg/mL solution are spread on an area of 704 cm^2. If all the VP monomers were in contact with the water surface then the total area occupied by VP monomers would be $A_{t,P2VP} = nN_{P2VP}a^2_{P2VP}\pi/4 \sim 505$ cm^2, where $N_{P2VP} = 1000$, monomer size $a_{P2VP} = 6.7$ Å, and n is a number of P_2VP chains in the spreading solution. Hence the observed onset area corresponds to the point where all the PVP blocks are on the surface and begin to contact each other. In the inset to Figure 1 we plot the onset area as a function of VP monomers in the spreading solution (dotted line). The solid line corresponds to the theoretical estimate obtained when all VP monomers were on the surface. The good agreement between the curves indicates that the PVP block is directly responsible for the surface pressure, even in the blends. If we now assume that the PVP block forms a stretched brush at the water interface, then the onset point of the plateau is a measure of the rigidity of this brush when the chains are forced to interdigitate. Hence as the number of surface P_2-VP chains decreases, the P_2VP chains become more flexible and the film becomes more collapsible.

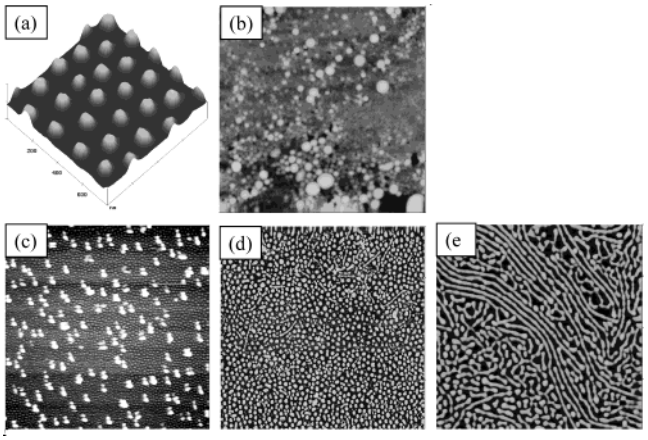

Figure 2. Morphology of LB film of different blends transferred at 10 dyn/cm for (a) PS-*b*-P_2VP; (b) PS-*b*-PF; (c) SF/SP = 1:2; (d) SF/SP = 2:1; (e) SF/SP = 4:1. AFM scan sizes are 10 × 10 μm^2 except for (a) in 1 × 1 μm^2.

The morphology of the monolayers as a function of blend composition, corresponding to the isotherms in Figure 1, was investigated by scanning force microscopy (SFM) in the contact mode. The monolayers were transferred from the water surface onto hydrophilic silicon wafers by the Langmuir−Blodgett (LB) technique. In Figure 2 we plot the morphologies of the film corresponding to the isotherms in Figure 1 at a surface pressure of 10 dyn/cm. In Figure 2a,b we plot films of pure PS-*b*-P_2VP and PS-*b*-PF diblocks, respectively. From the figure we see that the PS-*b*-P_2VP forms a highly ordered hexagonal lattice of spherical micelles, reported previously in refs 3, 9, and 10. Intermicellar spacing and height of the micelle are 150 and 12 nm, respectively, indicating that the PVP chains are fully stretched on the surface. In contrast, the PS-*b*-PF films show 3D aggregates with some spherical micelles of irregular size. In Figure 2c we show the morphology corresponding to the films with SF/SP ratio of 1/2 where we can see that the films are composed of an underlying hexagonal micelle lattice, similar to the one shown in Figure 2a, and an additional disordered phase that seems to be distributed across the lattice. Hence the disordered material appears to be the PS-*b*-PF copolymer that is mostly excluded from the ordered PS-*b*-P_2VP phase. Since the isotherm for this film (Figure

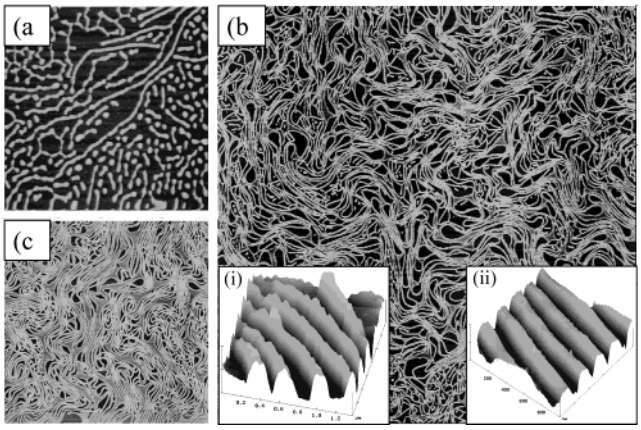

Figure 3. Morphology of LB film for SF/SP = 4:1 transferred at (a) 2 dyn/cm (10 × 10 μm^2), (b) 11 dyn/cm (30 × 30 μm^2), and its 3D image (1.4 × 1.4 μm^2) in inset (i). Inset (ii) in (b) shows 3D image (1.0 × 1.0 μm^2) after annealing at 150 °C for 24 h. (c) The morphology of SF/SP = 5:1 transferred at 11 dyn/cm (30 × 30 μm^2).

1b) exhibits a decreased onset area and onset point of plateau, we cannot rule out that some of the copolymer was incorporated. If we increase the PS-*b*-PF fraction further to where it is the majority component (SF/SP = 2:1) we find that a new ordered phase appears where cylindrical and spherical morphologies coexist. From Figure 1d we find that this phase is significantly softer than the previous phases and the plateau region nearly disappears. If the PS-*b*-PF fraction is increased further to 80%, the morphology becomes predominantly cylindrical (Figure 2e). This phase transition is qualitatively similar to that reported for diblock copolymers[2,5] when the volume fraction of the hydrophobic block increases from 50% to 90%.

We also explored the dependence of the surface morphologies on surface pressure and electric field. The results for the 4:1 blend are shown in Figure 3. From the figure we can see that at low pressures the morphology is predominantly spherical, while with increasing surface pressure to 11 dyn/cm the morphology is transformed into a dense network of "wires" whose dimension, as shown in the inset (i) in Figure 3b, is shown approximately 20 nm high and 150 nm wide. Increasing the SF ratio to 5:1 at 11 dyn/cm does not significantly change the structure, except that the width of the wire is increased to 300 nm as shown in Figure 3c. Application of an electric field in the plane of the surface, as shown in Figure 4a, caused the structures to compact further and produce a mesh. As can be seen from the figure, the spacing of the mesh decreased from 500 nm ∼ 1μm (Figure 4b) to 300 ∼ 500 nm (Figure 4c) with a change in the external field of 25 to 75 V/cm. This result was somewhat surprising since we had expected simply to orient the surface micelles along the field direction as previously reported for diblock copolymers in the melt.[1] Further work is currently in progress in order to better understand the mobility of polymer chains on a deformable surface in the presence of an electric field. On the other hand, annealing the LB films at 150°C for 24 h did not change the overall morphology but simply allowed the wire surface to become smoother in

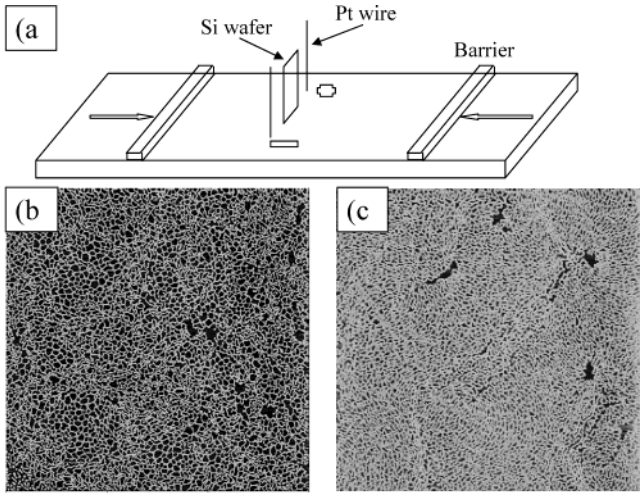

Figure 4. (a) Experimental setup of LB trough with the electric field. Two 0.1 mm platinum wires and a hydrophilic Si wafer with dimension (3 × 0.5) cm^2 were attached to the dipper. Pt wires were 1 cm apart from each other, and the Si wafer was placed in the middle. SPM images (30 × 30 μm^2) of SF/SP (4:1) film transferred at 11 dyn/cm, (b) under 25 V/cm, and (c) 75 V/cm.

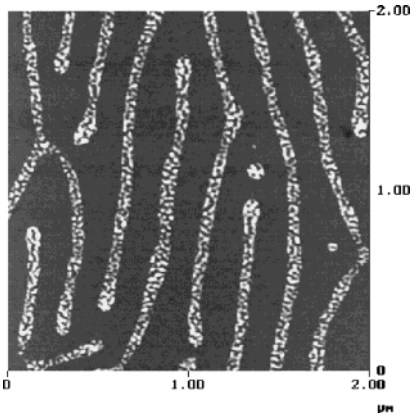

Figure 5. Oxygen reactive ion etching (O_2−RIE) on the LB film of SF/SP = 4:1 transferred at 10 dyn/cm (SPM images in 2 × 2 μm^2).

response to the increased surface pressure present at the air−water interface (see Figure 3b inset (ii)). This behavior is in contrast to that reported for block copolymers whose T_g is above room temperature and which exhibited very little motion in comparably low electric fields or in response to increased surface pressure. Films formed by these copolymers were thermally unstable and changed morphology after annealing for a few hours above their T_g.

To analyze distribution of SF copolymer in cylindrical domains, oxygen reactive ion etching (O_2−RIE), as well as Ar ion sputtering, was performed on LB films of SF/SP = (4:1) transferred at 10 dyn/cm (Figure 2e). Since the organometallic block has higher resistance than organic blocks to O_2 ion etching or Ar ion sputtering, the nanodomains of the organometallic part are resistant to removal by the plasma and hence can be imaged after etching.[11] The results are shown in Figure 5, which is a topographical image following O_2−RIE where we can see that the SF copolymer is incorporated into the spherical micelle hydrophobic core and where it forms a bicontinuous phase-separated pattern.

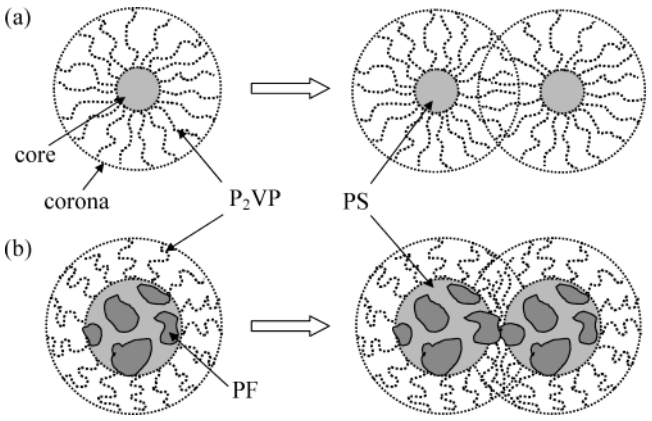

Figure 6. Schematic drawing of surface micelle of (a) pure PS-*b*-P_2VP with high coronal P_2VP chains density and (b) PS-*b*-PF/PS-*b*-P_2VP blends with low coronal chain density. With increasing surface pressure indicated by arrow, the cores in (b) are fused by PF blocks.

A simple model for the observed phenomena is sketched in Figure 6. When the spreading solution is in contact with the water substrate the block copolymer rapidly adsorbs to the water surface, and while there is still solvent remaining it self-assembles into surface micelles where one of the blocks forms a stretched brush in contact with the substrate while the other block aggregates into the core (Figure 6a). This organization can occur only while the solvent is still present and both blocks are mobile. Once the solvent evaporates, the core is vitrified and further motion is not possible. Increasing the surface pressure at this point simply forces the corona chains closer together, but has no effect on the overall morphology. As can be seen in Figure 6 and was described in ref 12, the micelle size is determined by balancing enthalpic and entropic interactions between the corona and the surface. Since the chains are already highly stretched, the film becomes rigid since the chains resist interdigitation with increasing surface pressure. When the FS copolymer is added, it is incorporated into the micelle core, but the ferrocene block is hydrophobic as well and cannot be incorporated into the PVP corona, which is stretched on the water surface. Hence addition of the FS copolymer increases the core size without increasing the grafting density of the corona (Figure 6b). This can be seen by comparing Figures 2c with 2d where the core increases from 100 to 300 nm, while the onset area which is a measure of compressibility decreases from 660 to 370 cm^2. The addition of the PS-*b*-PF copolymer also has the effect of plasticizing the films since T_g of this copolymer is in the vicinity of room temperature. Hence the chains remain mobile on the water surface even after evaporation of the solvent and can change their morphology in response to changes in surface density. The transition from spherical to cylindrical morphology with increasing surface concentration was first reported by Li et al.,[9] who studied the equilibrium surface morphologies as a function of concentration. They found that as the surface copolymer concentration increased, the micelle diameter decreased until finally the cores fused into cylinders. This configuration allowed more chains on the surface with minimum compression of the already extended corona. The ability of the films with large PS-*b*-PF fractions to reach their equilibrium configuration is further confirmed by the fact that further annealing to 150 °C for 24 h results only in "smoothing" of the wire surfaces but does not alter the overall morphology, as reported for the pure PS−PVP copolymer.[9]

In summary, we have shown that ordered structures can be induced in diblock copolymer blends, which would not occur if either of the copolymers was spread by itself. If T_g of one of the blocks is around the spreading temperature, the formed micelles retain their surface mobility and can organize into equilibrium structures in response to changes in surface density or applied electric field gradients. Hence, blending copolymers greatly increases the versatility of the structures that can be produced by the LB technique for nano- and meso-structured self-assembled polymer masks.

Acknowledgment. This work was supported by the NSF-MRSEC program.

References

(1) Thurn-Albrecht, T.; DeRouchey, J.; Russell, T. P.; Rainer, *Macromolecules* **2002**, *35*, 8106.
(2) Devereaux, C. A.; Baker, S. M. *Macromolecules* **2002**, *35*, 1921.
(3) Meli, M.; Badia, A.; Grutter, P.; Lennox, R. B. *Nano Lett* **2002**, *2*, 131.
(4) Li, Z.; Zhao, W.; Quinn, J.; Rafailovich, M. H.; Sokolov, J.; Lennox, R. B.; Eisenberg, A.; Wu, X. Z.; Kim, M. W.; Sinha, S. K.; Tolan, M. *Langnuir* **1995**, *11*, 4785.
(5) Meszaros, M.; Eisenberg, A.; Lennox, R. B. *Faraday Discuss.* **1994**, *98*, 283.
(6) Lammertink, R. G. H.; Versteeg, D. J.; Hempenius, M. A.; Vancso, G. J. *J. Polym. Sci., Part A* **1998**, *36*, 2147.
(7) Lammertink, R. G. H.; Hempenius, M. A.; Thomas, E. L.; Vancso, G. J. *J. Polym. Sci., Part B* **1999**, *37*, 1009.
(8) Manners, I. *Adv. Organomet. Chem.* **1995**, *37*, 131.
(9) Li, Z.; Zhao, W.; Liu, Y.; Rafailovich, M. H.; Sokolov, J.; Khougaz, K.; Eigenberg, A.; Lennox, R. B.; Krausch, G. *J. Am. Chem. Soc.* **1996**, *118*, 10892.
(10) Shin, K.; Rafailovich, M. H.; Sokolov, J.; Chang, D. M.; Cox, J. K.; Lennox, R. B.; Eisenberg, A.; Gibaud, A.; Huang, J.; Hsu, S. L.; Satija, S. K.; *Langmuir* **2001**, *17*, 4955.
(11) Lammertink, R. G. H.; Hempenius, M. A.; van den Enk, J. E.; Chan, V. Z.; Thomas, E. L.; Vancso, G. J. *Adv. Mater.* **2000**, *12*, 98.
(12) Kramarenko, E. Yu.; Potemkin, I. I.; Khokhlov, A. R.; Winkler, R. G.; Reineker, P. *Macromolecules* **1999**, *32*, 3495.

NL034917I